 DOI: 10.3217/978-3-85125-603-1-04

Early Predictors of Bone Infiltration in Multiple Myeloma Patients from T2 weighted MRI Images

Roxane Licandro[1,2], Johannes Hofmanninger[2], Marc-André Weber[3], Bjoern Menze[4], Georg Langs[2]
roxane.licandro@meduniwien.ac.at

***Abstract*— The analysis of bone infiltration patterns is a key issue in assessing the progression state of Multiple Myeloma (MM) and corresponding treatment response. MM is a blood affecting disease, that leads to an uncontrolled proliferation and malignant transformation of plasma cells and B-lymphocytes and ultimately can lead to osteolytic lesions first visible in Magnetic Resonance Imaging (MRI). It is particularly important to reliably assess lesions as early as possible, since they are a prime marker of disease advance and a trigger for treatment. However, their detection is difficult. Here, we present first results for the prediction of lesion progression based on longitudinal T2 weighted MRI imaging data. We evaluate a predictor for the identification of early signatures of emerging lesions, before they reach report thresholds. The algorithm is trained on longitudinal data, and visualizes high-risk locations in the skeleton.**

I. Introduction

Multiple Myeloma (MM) is a blood affecting malignancy of the bone marrow, that disturbes the generation pathway of plasma cells and B-lymphocytes and results in their uncontrolled proliferation and malignant transformation. Consequently, it leads to the alteration of bone remodelling mechanisms, by promoting bone resorption and inhibiting bone formation [9] and thus triggers the formation of focal or diffuse bone marrow infiltration. The gold standard for observing these initial infiltration patterns is MRI [1][7][4]. Subsequently, the progression of the disease leads to the building of osseous destructions, which are observable using low-dose Computer Tomography (CT) [5]. Figure 1 illustrates the infiltration pattern of a focal lesion evolving over four examination time points of a single patient. MM evolves over a precursor state of *Monoclonal Gammopathy of Undertmined Significance* (MGUS) and developes to an asymptomatic form of the disease called *smoldering Multiple Myeloma* (sMM), which progresses to the symptomatic form of MM [4]. Thus, it is particularly important to identify sMM patients of high risk of developing MM to enable early treatment [6]. Early detection includes the tracking of image positions over time to identify early signatures of their forming and to predict infiltration patterns of future disease states. The challenges here lie first in the accurate alignment of subject whole body images, second in imaging artefacts, and subtle non rigid deformations, and third in capturing the heterogeneity of diffuse infiltration patterns and their imaging signatures. Further variability is caused by different treatment strategies and patient specific treatment responses, and progression speed.

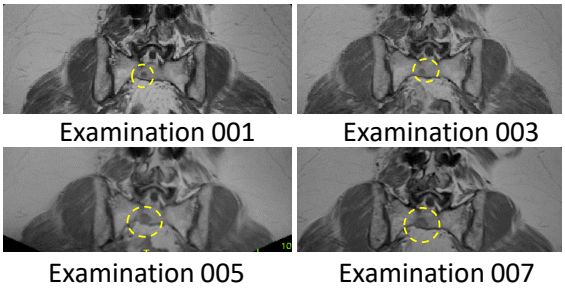

Fig. 1. Focal bone infiltration patterns are visible in MRI scans over multiple examination time points of one patient's sacrum.

A. Contribution

In this work we show and evaluate a predictor for future bone infiltration patterns oberserved in longitudinal T2 weighted MRI data. We propose a learning routine for a local predictor of lesion emergence and change, and show first results for prediction on T2 weighted MRI data. For providing predictive signatures of bone lesions, longitudinal relationships between subsequent stages of bone lesions and corresponding infiltration patterns of MM patients are assessed. The contribution of this work is three fold: (1) the longitudinal alignment of multiple bodyparts in whole body MRIs, (2) a classifier incorporating data from different disease stages in MM and (3) a probability prediction to identify bone regions evolving to diffuse or osteolytic lesions. An overview of the methodology proposed is given in Section II. The dataset and results of the evaluation are presented in Section III and this paper concludes in Section IV with an overview of possibilities for future work.

II. Methodology

In this section we summarize the processing steps for longitudinal alignment of T2 weighted MR images and the training for estimating a local lesion risk for future lesion emergence. In Figure 2 the computation pipeline proposed is visualised, which consists of a data acquisition component, data preprocessing component, a predictor training routine and a lesion risk score computation component.

[1] Department of Visual Computing and Human-centered Technologies - Computer Vision Lab, TU Wien; [2] Department of Biomedical Imaging and Image-guided Therapy - Computational Imaging Research Lab, Medical University of Vienna; [3] Department of Interventional and Diagnostic Radiology - Section Musco-Skelatal Imaging, Heidelberg University,; [4] Institute of Biomedical Engineering - Image-based biomedical modelling, Technische Universität München

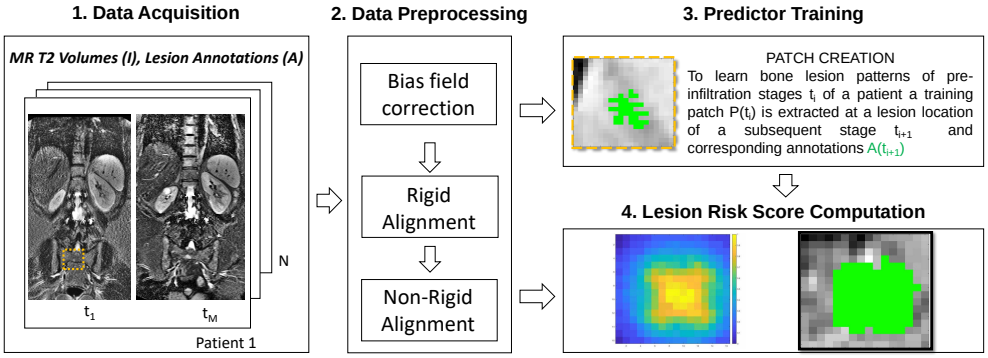

Fig. 2. Lesion Evolving Risk Computation Pipeline

A. Alignment of Longitudinal Acquisitions

The longitudinal analysis of subsequent lesion states of a subject requires precise registration of a patient's data $I_{t_i} = \{I_{t_1}, ...I_{t_M}\}$ over several examination time points t_i. In this a work a patient's image at a timepoint t_i is aligned to all subsequent timepoints $x = t_{i+1}, ..., t_M$, depending on the number of available data. We applied bias field correction before alignment using the FAST toolbox[1] [3] integrated in the FMRIB Software Library (FSL)[2]. The registration procedure is two fold: (1) Affine alignment is performed using a block matching approach for global registration (*reg_aladin*). (2) Non-rigid registration (*reg_f3d*) is performed to further transform the image of the affine registration step locally to the target at time point x. Both methodologies used are integrated in the NiftyReg toolbox[3] [8]. The performed registration offers accurate correspondences between follow-up images, which serves as basis for the extraction of imaging data depicting the development of bone infiltration and for the local lesion risk score calculation. The registered images were manually inspected if the lesions' position are in correspondence between examination time point. Figure 3 visualises a source scan of Patient 24 at examination time point 002 (left), the transformed source scan after affine registration (2nd column), the transformed source scan after affine + non-rigid registration (3rd column) and the target scan at examination time point 004 (middle).

B. Predictor Training Routine

In this study we used acquisitions from the body region of thorax, abdomen and pelvis (please cf. Section III for details regarding the dataset used). This area is considered, since most lesions occur there. For the application of a risk predictor we differentiate between the prediction of two lesion types: on the one hand lesions which *emerge* over time, i.e. which are not reported in the first scan, but in the subsequent scan, and on the other hand *growing* lesions, which are annotated in both observed examination time points. Image patches are extracted for every patient around a lesion's region longitudinally over following states. Two different patch sizes are evaluated within this work (8 × 4 × 8, 16 × 4 × 16 voxels with a voxelspacing of 1.302 mm × 6 mm × 1.302 mm). Data augmentation is performed by rotating every patch in steps of 20 degrees and randomly alternating the lesion location within the patch to obtain a higher number of training data and a more variable dataset. This results in *72 different patches per lesion*. To summarize, for 53 emerging lesions we obtain 3816 patches and for 44 growing lesions 3168 patches are created. For the generation of a test and training set, lesion wise leave one out cross validation is performed in such a way, that a testset consists of the 72 patches created from one single lesion and the training set of the remaining ones, i.e. in case of emerging lesions the testset would consist of 72 patches of one lesion and the train set of 3744 patches of the 52 remaining lesions.

C. Prediction of Local Lesion Evolving Risk

In this work we demonstrate the application of predicting future lesions and mark corresponding high risk locations, by incorporating knowledge from early signatures of emerging bone lesions to train a predictor. After the registration process the aligned T2 weighted MR images $I_{t_i}(I_{t_j})$ with corresponding subsequent time points t_j of the same patient lie in the same space of the target image I_{t_j} and corresponding annotation S_j of the lesion . In a next step these obtained pairs $(I_{t_i}(I_{t_j}), S_j)$ serve as basis for patch creation and subsequent training of a random forest classifier predicting future lesion labels from the present image data. This results in a score for each voxel position V expressing the probability determined by the trained random forest for a new input image.

III. RESULTS

In this section the dataset used for evaluation is presented and qualitative and quantitative results for the evaluation of the application of machine learning using random forests to predict lesion location is discussed.

A. Study Details

Within this study 220 longitudinal whole body (wb) MRIs from 63 patients with smoldering multiple myeloma were

[1] https://fsl.fmrib.ox.ac.uk/fsl/fslwiki/FAST [accessed 19th of February 2018]

[2] https://fsl.fmrib.ox.ac.uk/fsl/fslwiki/FSL [accessed 19th of February 2018]

[3] http://cmictig.cs.ucl.ac.uk/research/software/software-nifty/niftyreg [accessed 19th of February 2018]

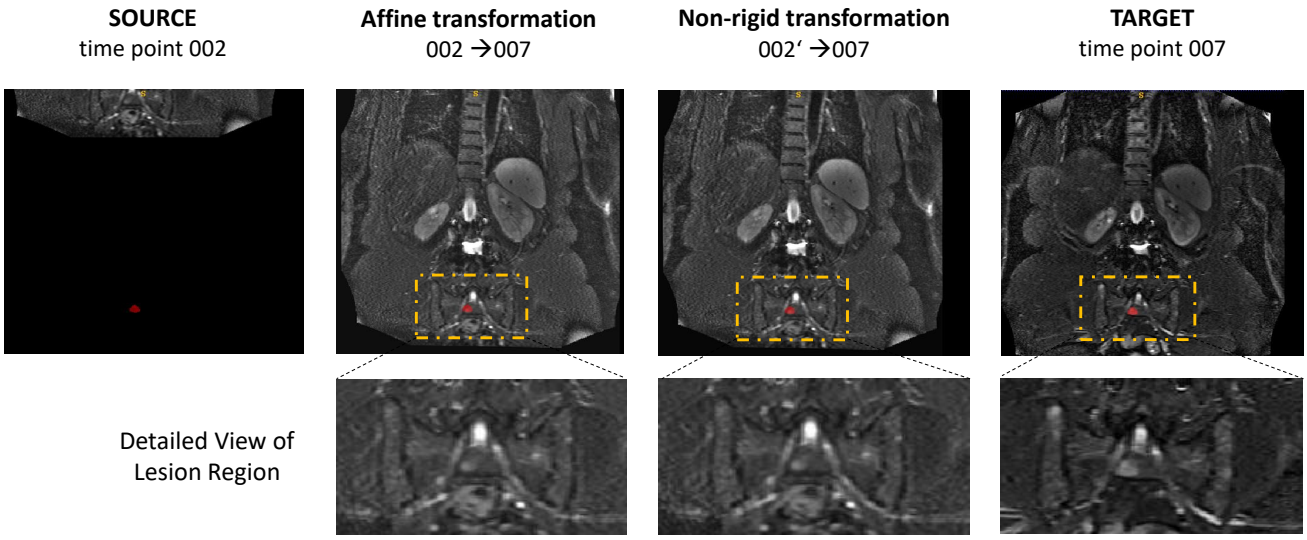

Fig. 3. Visualisation of the registration procedure of follow-up images of patient 24 from time point 002 to time point 007. The annotation of one lesion at time point 007 is visualised in red in all images in the first row. In the second row details of the lesion regions are illustrated.

TABLE I
DEMOGRAPHICS OF PARTICIPANTS

Patients	63 (39 male)
Age range (yrs)	29 -76
Median age at initial MRI (yrs)	55
Therapy	Radiation or resection
Median interval between MRIs	13 months
Median observation time	46 months

acquired between 2004 and 2011, following the 2003 guidelines [2]. At least one wbMRI was performed per patient. According to the IMWG consensus statement patients are considered to have symptomatic myeloma with the requirement of treatment, if more than one focal lesion with a diameter greater than 5 mm is present [1]. Thus, the focal lesions' annotation start at a lesion size bigger than 5 mm and is performed manually by medical experts. In Table I the demographics of the study participants is summarized. The protocol of this study was approved by the institutional ethics committee and all subjects gave their informed consent prior to inclusion. The scanning was performed on a 1.5 Tesla Magnetom Avanto (Siemens Healthineers, Erlangen, Germany) scanner. For the T2 weighted turbo-spin echo sequence (repetition time (TR):3340 ms milliseconds (ms), echo time (TE): 109 ms, section thickness (ST): 5 mm, acquisition time (TA): 2:30 min was performed of the head, thorax, abdomen, pelvis and legs using a coronal orientation. The duration of a scan was approximately 40 minutes long, no contrast medium was given.

B. Quantitative Evaluation Result of Lesion Risk Prediction

For the quantitative evaluation and for obtaining comparability between the different tested setups, the Area Under the ROC Curve (AUC) is computed, based on the probability estimates of the local lesion risk predictor for the test patch using scikit learn[4]. In Table II the mean AUC for emerging and growing lesion types are summarized. For every lesion type two different patch sizes are evaluated.

TABLE II
SUMMARY RESULTS

Lesion Type	Patch Size	Mean AUC
Emerging	8 x 4 x 8	0.904146
	16 x 4 x 16	0.8887
Growing	8 x 4 x 8	0.72949
	16 x 4 x 16	0.89803

C. Qualitative Evaluation Result of Lesion Risk Prediction

Figure 4 illustrates a prediction result for an emerging lesion. The test image (left) is a transformed image from examination time point 001 to 007 using the warping information obtain by the registration procedure introduced in Section 2. The extracted patch of this image in the region of the lesion visible in the target image I_{007} (right) is visualised in the first row in the center, with the predicted label in green and the annotation of the future lesion position extracted from image I_{007} in blue. In the second row the predicted probability map of the local lesion risk score is visualised, where orange shows regions of high probability and blue of low probability.

D. Discussion

For emerging lesions the mean AUC decreases with an increasing patch size. In contrast to this the mean AUC is increasing with increasing patch size for growing lesions. It is observable that emerging lesions achieve an approximately 0.20 higher mean AUC for the smaller patch size compared to similar mean AUC values for patches of size 16 x 4 x 16.

[4]http://scikit-learn.org/stable/auto_examples/model_selection/plot_roc.html[accessed 2nd of March 2018]

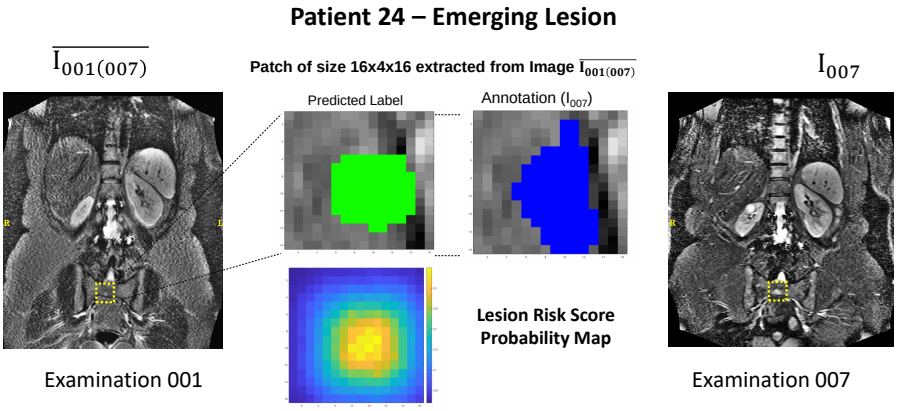

Fig. 4. Prediction of an emerging lesion from examination time point 001 to time point 007. The predicted label is visualised in green, below the underlying Local Lesion Risk Score probability map is shown and the manual annotation is visualised in blue.

IV. CONCLUSION

We presented an application of a classifier to predict a local lesion emergence risk for the analysis and visualisation of regions of high risk for bone lesions to emerge. A random forest predictor is trained using lesion image patches and annotations of subsequent lesions states of the longitudinal MR T2 weighted dataset. A challenge of this application is the accurate longitudinal alignment between images of subsequent examination time points of one patient. This is the first attempt to train a classifier to predict bone infiltration patterns in multiple myelome, while recent approaches are focusing on the detection and tracking (e.g. [10] for PET-CT) with deep learning techniques. So far the predictor is limited to image patches already located at approximate lesion locations focusing on the delineation of the lesions. We aim to adapt the proposed method to predict probability maps for entire images and different modalities. This will enable the longitudinal analysis of bone infiltration patterns caused by the progress of multiple myeloma.

ACKNOWLEDGMENTS

This work was supported by the DFG and the Austrian Science Fund (FWF) project number I2714-B31.

REFERENCES

[1] M. A. Dimopoulos, J. Hillengass, S. Usmani, E. Zamagni, S. Lentzsch, F. E. Davies, N. Raje, O. Sezer, S. Zweegman, J. Shah, A. Badros, K. Shimizu, P. Moreau, C.-S. Chim, J. J. Lahuerta, J. Hou, A. Jurczyszyn, H. Goldschmidt, P. Sonneveld, A. Palumbo, H. Ludwig, M. Cavo, B. Barlogie, K. Anderson, G. D. Roodman, S. V. Rajkumar, B. G. Durie, and E. Terpos, "Role of Magnetic Resonance Imaging in the Management of Patients With Multiple Myeloma: A Consensus Statement," *Journal of Clinical Oncology*, vol. 33, no. 6, pp. 657–664, feb 2015.

[2] B. G. M. Durie, R. A. Kyle, A. Belch, W. Bensinger, J. Blade, M. Boccadoro, J. Anthony Child, R. Comenzo, B. Djulbegovic, D. Fantl, G. Gahrton, J. Luc Harousseau, V. Hungria, D. Joshua, H. Ludwig, J. Mehta, A. Rodrique Morales, G. Morgan, A. Nouel, M. Oken, R. Powles, D. Roodman, J. San Miguel, K. Shimizu, S. Singhal, B. Sirohi, P. Sonneveld, G. Tricot, B. Van Ness, and Scientific Advisors of the International Myeloma Foundation, "Myeloma management guidelines: a consensus report from the Scientific Advisors of the International Myeloma Foundation," *The Hematology Journal*, vol. 4, no. 6, pp. 379–398, 2003.

[3] M. Jenkinson, C. F. Beckmann, T. E. J. Behrens, M. W. Woolrich, and S. M. Smith, "FSL." *NeuroImage*, vol. 62, no. 2, pp. 782–90, aug 2012.

[4] J. K. Kloth, J. Hillengass, K. Listl, K. Kilk, T. Hielscher, O. Landgren, S. Delorme, H. Goldschmidt, H.-U. Kauczor, and M.-A. Weber, "Appearance of monoclonal plasma cell diseases in whole-body magnetic resonance imaging and correlation with parameters of disease activity," *International Journal of Cancer*, vol. 135, no. 10, pp. 2380–2386, nov 2014.

[5] L. Lambert, P. Ourednicek, Z. Meckova, G. Gavelli, J. Straub, and I. Spicka, "Whole-body low-dose computed tomography in multiple myeloma staging: Superior diagnostic performance in the detection of bone lesions, vertebral compression fractures, rib fractures and extraskeletal findings compared to radiography with similar radiation," *Oncology letters*, vol. 13, no. 4, pp. 2490–2494, apr 2017.

[6] M.-V. Mateos, M.-T. Hernández, P. Giraldo, J. de la Rubia, F. de Arriba, L. L. Corral, L. Rosiñol, B. Paiva, L. Palomera, J. Bargay, A. Oriol, F. Prosper, J. López, J.-M. Arguiñano, N. Quintana, J.-L. García, J. Bladé, J.-J. Lahuerta, and J.-F. S. Miguel, "Lenalidomide plus dexamethasone versus observation in patients with high-risk smouldering multiple myeloma (QuiRedex): long-term follow-up of a randomised, controlled, phase 3 trial." *The Lancet. Oncology*, vol. 17, no. 8, pp. 1127–1136, aug 2016.

[7] M. Merz, T. Hielscher, B. Wagner, S. Sauer, S. Shah, M. S. Raab, A. Jauch, K. Neben, D. Hose, G. Egerer, M.-A. Weber, S. Delorme, H. Goldschmidt, and J. Hillengass, "Predictive value of longitudinal whole-body magnetic resonance imaging in patients with smoldering multiple myeloma," *Leukemia*, vol. 28, no. 9, pp. 1902–1908, sep 2014. [Online]. Available: http://www.ncbi.nlm.nih.gov/pubmed/24535407http://www.nature.com/doifinder/10.1038/leu.2014.75

[8] M. Modat, D. M. Cash, P. Daga, G. P. Winston, J. S. Duncan, and S. Ourselin, "Global image registration using a symmetric block-matching approach." *Journal of medical imaging (Bellingham, Wash.)*, vol. 1, no. 2, p. 024003, jul 2014.

[9] P. Tosi, "Diagnosis and treatment of bone disease in multiple myeloma: spotlight on spinal involvement." *Scientifica*, vol. 2013, p. 104546, dec 2013.

[10] L. Xu, G. Tetteh, J. Lipkova, Y. Zhao, H. Li, P. Christ, M. Piraud, A. Buck, K. Shi, and B. H. Menze, "Automated Whole-Body Bone Lesion Detection for Multiple Myeloma on 68 Ga-Pentixafor PET/CT Imaging Using Deep Learning Methods," *Contrast Media & Molecular Imaging*, vol. 2018, pp. 1–11, jan 2018.